

This is an author produced version of a paper published in
Dalton Transactions.

This paper has been peer-reviewed but may not include the final publisher
proof-corrections or pagination.

Citation for the published paper:

Lars Eklund, Tomas S. Hofer and Ingmar Persson. (2015) Structure and water
exchange of hydrated oxo halo ions in aqueous solution using QMCF MD
simulation, large angle X-ray scattering and EXAFS. *Dalton Transactions*.
Volume: 44, Number: 4, pp 1816-1828.
<http://dx.doi.org/10.1039/c4dt02580f>.

Access to the published version may require journal subscription.
Published with permission from: Royal Society of Chemistry.

Epsilon Open Archive <http://epsilon.slu.se>

Structure and water exchange dynamics of hydrated oxo halo ions in aqueous solution using QMCF MD simulation, large angle X-ray scattering and EXAFS

Lars Eklund,^a Tomas S. Hofer,^b and Ingmar Persson^{a,*}

^a Department of Chemistry and Biotechnology, Swedish University of Agricultural Sciences, P.O.Box 7015, SE-750 07 Uppsala, Sweden,

^b Theoretical Chemistry Division, Institute of General, Inorganic and Theoretical Chemistry, University of Innsbruck, Innrain 80-82, A-6020 Innsbruck, Austria.

E-mail: ingmar.persson@slu.se

† Electronic supplementary information (ESI) available: bond lengths in selected solid chlorite, chlorate, bromite, bromate, perbromate, iodate and periodate salts, radial distribution functions of the hydrated chlorite, chlorate and perchlorate ion from QMCF MD simulations, RDFs and intensity function from LAXS measurements on aqueous solutions on sodium bromate, iodate and metaperiodate, and fitted EXAFS data and Fourier transforms on sodium meta- and orthoperiodate in solid state and aqueous solution. See DOI: 10.1039/xxxxxxx

Abstract

Theoretical *ab initio* quantum mechanical charge field molecular dynamics (QMCF MD) has been applied in conjunction with experimental large angle X-ray scattering (LAXS) and EXAFS measurements to study structure and dynamics of the hydrated oxo chloro anions chlorite, ClO_2^- , chlorate, ClO_3^- , and perchlorate, ClO_4^- . In addition, the structures of the hydrated hypochlorite, ClO^- , bromate, BrO_3^- , iodate, IO_3^- and metaperiodate, IO_4^- , ions have been determined in aqueous solution by means of LAXS. The structures of the bromate, metaperiodate, and orthoperiodate, $\text{H}_2\text{IO}_6^{3-}$, ions have been determined by EXAFS as solid sodium salts and in aqueous solution as well. The results show clearly that the only form of periodate present in aqueous solution is metaperiodate. The Cl-O bond distances in the hydrated oxo chloro anions as determined by LAXS and obtained in the QMCF MD simulations are in excellent agreement, being 0.01-0.02 Å longer than in solid anhydrous salts due to hydration through hydrogen bonding to water molecules. The oxo halo anions, all with unit negative charge, have low charge density making them typical structure breakers, thus the hydrogen bonds formed to the hydrating water molecules are weaker and more short-lived than those between water molecules in pure water. The water exchange mechanism of the oxo chloro anions resembles those of the oxo sulfur anions with a direct exchange at the oxygen atoms for perchlorate and sulfate. The water exchange rate for the perchlorate ion is significantly faster, $\tau_{0.5}=1.4$ ps, compared to the hydrated sulfate ion and pure water, $\tau_{0.5}=2.6$ and 1.7 ps, respectively. The angular radial distribution functions show that the chlorate and sulfite ions have a more complex water exchange mechanism. As the chlorite and chlorate ions are more weakly hydrated than the sulfite ion the spatial occupancy is less well-defined and it is not possible to follow any well-defined migration pattern as it is difficult to distinguish between hydrating water molecules and bulk water in the region close to the ions.

Introduction

The physico-chemical properties and the reaction rates of chemical species in solution are largely dependent on their interactions with the solvent. In this respect, most metal ions are thoroughly studied in aqueous solution with experimental¹⁻³ as well as theoretical simulation studies.⁴⁻⁶ On the other hand, the number of such studies of anions is scarce, and among the oxo anions studied with both simulations and experimental structure determination in aqueous solution includes only sulfate, selenate, sulfite, thiosulfate and chromate.⁷⁻¹² An experimental difficulty with hydrated anions is that the hydrogen bonds to the hydrating water molecules are relatively weak, and the exchange rates are normally faster than allowed to be studied with the experimental methods available today. Theoretical simulation is therefore an option to obtain information about water exchange mechanism and dynamics, as well as structure, of hydrated anions in aqueous solution. The experimental structure determination of anions in aqueous solution has to be performed with large angle X-ray scattering (LAXS) or large angle neutron scattering (LANS), which are sensitive to long distances as those between anions and hydrating water molecules, while e.g. EXAFS is not applicable as it is not sensitive enough to such distances, and only the bond distance with e.g. an oxo anion can be determined accurately.¹³

The structure and water exchange mechanism of the hydrated oxo sulfur anions, sulfate, sulfite and thiosulfate, have recently been studied in combined *ab initio* quantum mechanical charge field molecular dynamics (QMCF MD) simulations and experimental LAXS studies.⁸⁻¹⁰ These studies showed that structures of hydrated anions in aqueous solution can be determined accurately with LAXS, and that simulations give in principle identical results. Each oxygen atom in the sulfate, sulfite and thiosulfate ions, and the terminal sulfur atom in the latter, form hydrogen bonds to three hydrating water molecules, Figure 1.⁸⁻¹⁰ The hydration causes the S-O and S-S bond distances to become slightly longer, 0.01-0.02 Å, in aqueous solution compared with the distance in anhydrous solids.⁸⁻¹⁰ Weak electrostatic interactions are formed between the lone electron-pair on the sulfite ion and the water molecules clustered outside it, Figure 1, left panel. Simulations give also

information about the water exchange mechanism and rate. The water exchange rates of anions are very fast, in the ps regime, and the water exchange mechanism may differ significantly between different anions as found for the sulfate and thiosulfate ions on one hand, and the sulfite ion, with a lone electron-pair, on the other.^{8,10} The sulfate and thiosulfate ions exchange water molecules directly at the oxygens, and at the terminal sulfur in thiosulfate, with exchange rates, $\tau_{0.5}$, of 2.6 and 2.25/1.16 (oxygens/sulfur) ps, respectively,^{8,10} compared to 1.7 ps in pure water.¹⁸ On the other hand, the angular radial distribution function (ARD) shows that the sulfite ion has a much more complex mechanism. The water exchange takes place in close vicinity of the lone electron-pair directed at the sides, while in principle no water exchange takes place at the sulfite oxygens during the time of the simulation.⁹ Double difference infrared spectroscopy have shown that the oxo sulfur anions, with -2 charge, form stronger hydrogen bonds to the hydrating water molecules and with longer mean residence time (MRT) than those in pure water, Figure 1.³ The oxo sulfur anions are therefore regarded as structure making anions. The opposite is found for anions with the charge -1, except the fluoride ion, and such anions are consequently regarded as structure breaking anions.³

The oxo halo acids, hypochlorous, HClO, chlorous, HClO₂, chloric, HClO₃, and perchloric, HClO₄, acid, and their salts are widely used in many daily and technical applications normally in the form of aqueous solutions.¹⁵ Hypochlorous acid is a relatively strong oxidizer, which cannot be isolated in the pure form as it decomposes to chlorine when dissolved in water. Aqueous solutions of the corresponding sodium and calcium salts, hypochlorites, are frequently used as bleach, deodorants and disinfectants. Chlorous acid is also unstable as it disproportionates to hypochlorous and chloric acid which in large parts counteracts its oxidizing properties. Also in this case the corresponding anion, chlorite, is stable and the main use of the sodium salt in aqueous solution is the production of chlorine dioxide, which is a strong oxidizing agent used in water treatment and bleaching. Chloric acid is a relatively strong acid, $pK_a \approx 1$,¹⁶ a strong oxidizing agent, but it is never stable as it disproportionates according to several routes depending on conditions. Chlorate salts are powerful oxidizing agents and must be kept away from organics or easily oxidized materials.

Mixtures of chlorate salts with virtually any combustible material, such as sugar, sawdust, charcoal, organic solvents, metals, etc., will readily deflagrate or explode. However, aqueous solutions of chlorates are more stable but should be handled with care. Perchloric acid is a strong acid, completely dissociated in aqueous solution, and a strong oxidizing agent. Perchloric acid is dangerously corrosive and readily forms potentially explosive mixtures with many organic compounds.

Perchloric acid and perchlorate salts are normally safe as aqueous solutions. Perchlorate salts are commonly used as inert salts in physico-chemical studies as the perchlorate ion is in most cases inert to form chemical interactions to other chemical species in aqueous solution. Bromic acid and bromates are powerful oxidizing agents and are common ingredients in Belousov-Zhanotinsky reactions.¹⁷ Bromate has properties similar to chlorate, but is a weaker oxidizing agent. Iodic acid is stable in its pure form, and a relative strong acid in aqueous solution, $pK_a=0.75$,¹⁶ with oxidizing properties, especially in acidic solution. Periodic acid and periodates can exist in the forms meta, HIO_4 and IO_4^- , and ortho, H_5IO_6 and IO_6^{5-} , respectively. Periodates can cleave carbon-carbon bonds in a variety of 1,2-difunctionalised alkanes, with the most common example being diol cleavage.¹⁸

The aim of this study is to analyse the hydration of the oxo chloro anions chlorite, chlorate and perchlorate in aqueous solution using a combination of *ab initio* QMCF MD simulations and LAXS experiments. The low charge density of the mono-charged oxo chloro anions causes these anions to act as structure breakers, and the water exchange rate of these ions is of the same order of magnitude or slightly faster than in pure water. This has already been established by experimental DDIR and LAXS studies in aqueous solution for the perchlorate ion.^{19,20} It is of particular interest to compare the hydration of the corresponding oxo sulfur and oxo halo anions from a water exchange point of view as they are known/expected to be structure makers and breakers, respectively, and whether the lone electron-pair(s) on the chlorite and chlorate ions is causing the same dramatic change in water exchange mechanism as it does on the sulfite ion. The structures of the hydrated hypochlorite, bromate, iodate and periodate ions in aqueous solution have been determined by LAXS as well. Furthermore, EXAFS studies have been performed on the two forms of periodate,

meta and ortho, in solid state and aqueous solution to determine whether both forms or only one of them is stable in aqueous solution.

Experimental

Chemicals. Sodium chlorate, NaClO₃ (Sigma-Aldrich, >99%), perchloric acid, HClO₄ (Sigma-Aldrich, 70 weight%), sodium bromate, NaBrO₃ (Sigma-Aldrich, >99%), sodium iodate, NaIO₃ (Sigma-Aldrich, >99%), sodium metaperiodate, NaIO₄ (Sigma-Aldrich, >99%), and trisodium orthoperiodate, Na₃H₂IO₆ (Sigma-Aldrich, >99.9%), were used without further purification. Sodium chlorite (80%), NaClO₂, was recrystallized from water and gently dried before preparation of the solution. Sodium hypochlorite was purchased as an aqueous solution, checked to be 15.0 weight% from the measured density, and stored in refrigerator until use.

Solutions. The solutions for the LAXS and EXAFS experiments were prepared by dissolving weighed amounts of the salts in Milli Q filtered water, and pH was adjusted to a value above 7.0 by addition of a small amount of sodium hydroxide if necessary. The perchloric acid was diluted with Milli Q filtered water to the desired concentration. The concentrations of all ions and water for all solutions studied by LAXS and EXAFS are summarized in Table 1.

Large Angle X-ray Scattering (LAXS). The scattering of MoK α X-ray radiation, $\lambda=0.7107\text{ \AA}$, from the free surfaces of the aqueous solutions was measured in a large angle Θ - Θ goniometer described elsewhere.²¹ A flat measuring surface of the irradiated area was obtained by filling a Teflon cup until a positive meniscus was observed and it was sealed from the atmosphere by an airtight measuring chamber with beryllium windows. A LiF(200) single crystal focusing monochromator was used to monochromatise the scattered radiation. The scattering was determined at 450 discrete angles in the angle range $0.5 < \Theta < 65^\circ$, where the scattering angle is 2Θ . 100,000 X-ray quanta were collected for each angle, and the entire angle range was scanned twice corresponding to a statistical error of about 0.3 %. A combination of divergence-collecting-focal slits of $1/4^\circ$ - $1/2^\circ$ -0.1 mm and 1° - 2° -0.2 mm defining the X-ray beam were applied with the smaller slits

for $\Theta < 13^\circ$ and the larger for $\Theta > 10^\circ$. To get a suitable counting rate and change in angle, data was collected in three different Θ -regions, with overlapping regions to enable scaling of the data. The details of data collection and treatment are described elsewhere.²¹ The KURVLR software²² was used for the data treatment. The structural parameters contained in the theoretical model were refined by minimizing $U = w(s)\sum s^2[i_{\text{exp}}(s) - i_{\text{calc}}(s)]^2$ using the STEPLR program.^{23,24} Normalisation of the data to one stoichiometric unit containing one halogen atom was made by the use of the scattering factors f for neutral atoms, including corrections for anomalous dispersion, $\Delta f'$ and $\Delta f''$,²⁵ Compton scattering^{16,17} and multiple scattering events. The multiple scattering events play a significant role in the scatter from solutions with low molar absorption coefficient, $\mu < 15 \text{ cm}^{-1}$, which has been corrected for; the μ values are given for respective solution in Table 1. To make peak widths comparable with data from the QM/MD simulations the temperature factors were recalculated as full width half height, fwhh, assuming Gaussian distributed peaks, then $b=l^2/2$ gives $\text{fwhh}=\sqrt{(\ln 2)*2}*\sqrt{(2*b)}$.

EXAFS. Bromine and iodine K-edge X-ray absorption spectra of solid and aqueous solutions of sodium bromate, meta- and orthoperiodate, as listed in Table 1, were collected at the wiggler beam-line 4-1 at Stanford Synchrotron Radiation Lightsource (SSRL), Stanford University, USA. The facility operated at 3.0 GeV and a current of 500 mA run in top-up mode. A double crystal Si(220) monochromator was used. The second monochromator crystal was detuned to 60 and 80% of maximum intensity at the end of the scans for bromine and iodine EXAFS data, respectively, to minimize higher harmonics. The solutions were contained in cells made of 1.5 and 5.0 mm Teflon spacers for bromate and iodate/periodates, respectively, and 6 μm polypropylene film hold together with titanium frames. The solids, diluted and carefully mixed and ground with boron nitride, were contained in 1.5 mm thick aluminum frames covered with tape. The experiments were performed in transmission mode using ion chambers with a gentle flow of nitrogen and argon, respectively. The energy scale of the X-ray absorption spectra was calibrated by assigning the first inflection point of the K edge of finely ground sodium bromide and iodine samples to 13474 and 33168 eV,

respectively.²⁸ For each sample 3 scans were averaged, giving satisfactory data (k^3 -weighted) in the k range 2-13 Å⁻¹. Data treatment was performed with the computer program package EXAFSPAK.²⁹ *Ab initio* calculated phase and amplitude parameters, used by the EXAFSPAK program, were computed by the FEFF7 program.³⁰ The standard deviations reported for the refined parameters in Table 2 were obtained from least squares refinements of the k^3 weighted EXAFS function, $\chi(k) \cdot k^3$, and do not include systematic errors of the measurements. These statistical error values allow reasonable comparisons of e.g. the significance when comparing relative shifts in the distances. However, variations in the refined parameters, including the shift in the E_0 value (for which $k = 0$), using different models and data ranges, indicate that the absolute accuracy of the distances given for the separate complexes is within ±0.005 to 0.02 Å for well-defined interactions. The “estimated standard deviations” given in the text have been increased accordingly to include estimated additional effects of systematic errors.

Quantum Mechanical Charge Field Molecular Dynamics (QMCF MD)

The simulation systems were separated into a high- and a low-level zone, to enable the use of a hybrid quantum mechanical/molecular mechanical (QM/MM) approach.³¹⁻³⁷ To accurately describe the interactions, molecules in the closest region to the solute are treated by application of a suitable quantum chemical technique while classical potential functions are considered sufficient for the description of the remaining part of the system. In addition the QMCF approach exploits the fact that non-Coulombic interactions become negligible at relatively short distances.^{38,39} This means that for atoms located in the centre of the quantum mechanical region, the application of these non-Coulombic contributions in the QM/MM coupling can be safely neglected, provided that the size of the QM region is sufficiently large. Thus, the QM region is further separated into a core and layer zone. This separation is done because near the QM/MM border the pair distances again become small and therefore, the non-Coulombic interactions must be explicitly handled in addition to the Coulombic contribution. Since all molecules in the layer region are solvent molecules the non-Coulombic interaction can be handled as for solvent-to-solvent interactions in the MM region. In

addition, the application of the electrostatic embedding technique to account for the influence of the partial charges of the atoms in the MM region surrounding the quantum mechanical zone was found to greatly improve the description of the system.^{38,39} The migration of molecules between the high- and low-level zone requires that the use of a smoothing procedure is applied to continuously shift the forces from the QM to MM contribution and *vice versa*. Further information on the QMCF technique is given in detail elsewhere.³⁸⁻⁴⁰

Simulation protocol. A periodic boundary condition was used in a cubic box with an edge length of 31.4 Å containing 1000 water molecules, corresponding to a density of 0.997 g·cm⁻³. The target temperature of 298 K was kept constant via the Berendsen weak coupling algorithm.⁴¹ The Coulombic cut-off was set to 12.0 Å. To account for the error associated with the use of a Coulombic cut-off, the reaction field approach was employed.⁴² The classical equations of motion were treated via the velocity Verlet algorithm⁴³ with a time-step of 0.2 fs, recording data every fifth time-step. Based on their centres of mass, molecules within a radius of 7.3 Å from the chlorine atom are included into the QM region. This distance was chosen using information from the LAXS measurements of the chlorite, chlorate and perchlorate ions, considering the distances to the water molecules clustered outside the solute's oxygen atoms. By this selection it is secured that the complete hydration shells are treated quantum mechanically at the Hartree-Fock/Dunning double zeta plus polarisation (DZP) level.^{44,45} In the past the HF approach was successfully employed in QMCF MD simulation studies of hydrated sulfate, sulfite and thiosulfate ions.⁸⁻¹⁰ The simple model produced a good result and sufficient number of simulation steps within a reasonable production time of one year, running on 4 AMD Opteron 2382 quad-core processor (16 cores). The success of the method on those systems motivates the use of the methodology also in this study. The quantum chemical computations were executed with the TURBOMOLE 6.4 software package.⁴⁶ To describe the solvent-solvent interaction between molecules in the MM region as well as in the QM/MM coupling the flexible BJH-CF2 water model was used,^{47,48} since it explicitly takes intramolecular hydrogen modes into account. The simulation ran ca. 6.6, 7.4 and 8.0 ps for equilibration, the length

of the sampling period was 12.5, 11.7 and 14.5 ps for the hydrated chlorite, chlorate and perchlorate ions, respectively.

Analysis methods of the QMCF simulation

The simulation trajectory has been analysed in terms of radial distribution functions (RDFs), angular-radial-distributions (ARDs), coordination number (CN) distribution and mean lifetime analysis of ligand exchange. Typically, the RDF obtained from simulations is expressed as $g(r) = V/N^2 \langle n(r, \Delta r) \rangle_M / 4\pi\rho_0 r^2 \Delta r$, while the experimental RDF is given as $D(r) - 4\pi\rho_0 r^2$. Using angularly overlapping conical regions with a central vector along the C_{3v} axis a function of distance and angle, $D(r, \alpha)$, an ARD is defined³⁹ where α is the angle of the conical region with respect to the central axis, in these cases the step in α was 22.5°. The ARD can then be used to compare water distributions of the hydration sphere with other ions.

To estimate the coordination number distribution each water oxygen atom within the respective first shell distance of the oxygen and/or chlorine atoms of the solute species has been registered in each frame of the simulation. The respective average corresponds to the total coordination number of the solute.

Mean ligand residence times (MRTs), τ , were analysed using a direct measurement of exchange events.¹⁸ By registering all border crossing events $N_{ex}^{0.5}$ lasting for a duration of $t^* = 0.5$ ps,¹⁸ the mean residence time is obtained as $\tau_{0.5} = CN_{av} N_{ex}^{0.5} / t_{sim}$ where CN_{av} and t_{sim} correspond to the average coordination number and the total simulation time, respectively. The ratio of exchanges R_{ex} obtained as the ratio of the number of registered exchange events and the number of all occurring border crossings $N_{ex}^{0.0}$ (registered for $t^* = 0.0$ ps) corresponds to the average number of border crossing attempts to achieve one lasting exchange event. Visual modelling was conducted using VMD.⁴⁹

Results and Discussion

Structure of the chlorite, chlorate and perchlorate ions in aqueous solution

The experimental RDFs from the LAXS measurements of the aqueous solutions of sodium chlorite and chlorate and of perchloric acid show peaks at ca. 1.5, 2.9 and 3.9 Å, Figures 2, S1 and S2†. The weak peak at 1.45-1.6 Å corresponds to the Cl-O bond distance, and the peak at ca. 3.8 Å to the Cl(-O)…O_{aq} distance. The strong peak at 2.9 Å contains two contributions, the (Cl-)O…O_{aq} distance, and the mean O_{aq}…O_{aq} distance in the aqueous bulk, Figures 2, S1 and S2†. The refined distances are given in Table 2. The Cl-O bond distances are slightly longer in aqueous solution, 0.01-0.02 Å, than in anhydrous solids, Table S1†, due to hydration effects of the formed hydrogen bonds. The refined Cl-O, (Cl-)O…O_{aq} and Cl(-O)…O_{aq} distances show that the Cl-O…O_{aq} bond angle is very close to 109.5 °, showing a tetrahedral configuration around the chlorite, chlorate and perchlorate oxygens and that most likely on average three water molecules are hydrogen bonded to each oxygen. The structure of the hydrated sodium ion was modelled as a regular octahedron with a mean Na-O bond distance of 2.43(2) Å, which is in full agreement with previously reported distance.⁵⁰ The structure of the oxonium ion in the perchloric acid solution gives only a very weak contribution to the RDF and any well-defined structure cannot be evaluated. There is a very weak shoulder around 2.5 Å which may be an O(-H)…O interaction between the first and second hydration sphere in the hydrated oxonium ion which is expected to be very strong and with a distance of 2.5-2.6 Å.^{51,52} However, it has not been included in the model as it is too weak and not unambiguous. The experimental and the calculated RDFs and the refined intensity functions using the parameters given in Table 2 are shown in Figures 2, S1 and S2† together with the individual contributions from the hydrated chlorite, chlorate, perchlorate and sodium ions, and the aqueous bulk.

The RDF analysis of the QMCF MD simulation resulted in structure parameters in excellent agreement with the experimental ones, Table 2 and Figure S3†. The bond distance distribution is somewhat narrower for the high populated distances of the oxygens of the central ion compared to

experiment, but as expected the low populated longer distances in the hydration shells become broader and less well defined in the simulation due to shorter average time than in the experiment.

Water exchange dynamics of the chlorite, chlorate and perchlorate ions in aqueous solution

The ARD for a plane cutting though the ion parallel to an axis of symmetry shows the distribution of distances as a function of angle. The $g(r,\alpha)_{\text{Cl-O}}$ is the population of water oxygens at a certain distance and angle to the plane vector centred on Cl, Figure 3. For the perchlorate ion (Figure 3, right panel) a narrow symmetric distribution in both distance and angle for a large value of $g(r)_{\text{Cl-O}}$ show a symmetric exchange with a diffuse and distributed hydration shell with low population. There is a distinct difference in the distribution function of the hydration shell of the chlorate and chlorite ions (Figure 3, middle and left panel, respectively) as compared to the perchlorate ion. The chlorate ion display an asymmetric distribution of the minima outside of the hydration shell similar to the sulfite ion.¹⁰ However, the effect is much weaker due to the lower charge density on the chlorate ion. Fitting of the hydrogen bond correlation functions gave hydrogen bond lifetimes for O···H-O_{aq} of 0.42, 0.16 and 0.14 ps for ClO₂⁻, ClO₃⁻ and ClO₄⁻, respectively, Table 3 and Figure 4. The hydrogen bond lifetime of Cl···H-OH_{aq} was found to be 0.24 and 0.11 ps for ClO₂⁻ and ClO₃⁻, respectively, Table 3 and Figure 4. This shows that the hydrogen bond interactions to the chlorite and chlorate ions are significantly different, with water-oxygen hydrogen bonds lasting on average 1.8 and 1.5 times longer than hydrogen bonds to chlorine in the respective ions, Tables 4 and 5. An MRT is obtained by selecting a region from minimum to minimum in the hydration shell distance from Cl. This will of course not reflect the distribution of exchange events but rather just the total number of them between the hydration shell and bulk water. The MRT is compiled in Tables 4 and 5, and it is seen that the chlorite and perchlorate ions clearly are structure breakers with MRTs of 1.6 and 1.4 ps, respectively. The MRT of the chlorate ion suggests that it is a weak structure maker at 2.05 ps. This probable over-estimation was most likely caused by the short simulation time with respect to the MRT analysis and the spherical cut-off used with the MRT, as shown in the case of sulfite,¹⁴ which become

problematic if the central atom has asymmetrical interactions and not a direct water exchange at the oxygen atom. From the hydrogen bond lifetimes it was shown that the chlorate ion has a significant difference in hydrogen bond interaction across the ion with the hydrogen bonds lasting 1.5 times longer when interacting with the oxygens as with the chlorine. However, by studying the structural data with respect to the hydrated chlorate ion effect on the bulk water, along with the hydrogen bond structure and ARD results it can be concluded that the chlorate ion most likely is a weak structure breaker.

The coordination number distributions of the three different systems are depicted in Figure 5. The distributions show similar broadness with intensities for the most populated CN 10, 11 and 12 for chlorite, chlorate and perchlorate amounting to 27, 29 and 24%, respectively. Overall an increase in the number of coordinating water molecules can be observed with average coordination numbers amounting to 9.8, 11.1 and 12.0 for chlorite, chlorate and perchlorate, respectively, which agree well with the data obtained via experiment. Using the results from the LAXS studies, on average three water molecules are hydrogen bonded to the perchlorate, chlorate and chlorite oxygens, whereas on average two water molecules are clustered outside the lone electron-pair(s) on chlorine in the hydrated chlorate and chlorite ions.

To highlight the hydration pattern in more detail spatial density plots of water oxygen atoms have been generated after alignment of the solutes to their respective reference geometries based on the average bond distances and valence angles observed along the simulation, Figure 6. Although no density information can be obtained in the depiction of an iso-surface, the three-dimensional arrangement of ligands can be discussed in a straightforward way.

In case of the chlorite system the oxygen coordination occurs in small defined volumes, while for the chlorine atom a more distributed coordination pattern is observed. This oxygen distribution is in line with the rather long hydrogen bond life times observed for the ClO_2^- oxygen atoms compared to the chlorine atom, Figure 6a. For chlorate a similar behavior near the oxygen atoms is

observed, however, since the solute charge is now distributed over one more atom, the spatial density pattern is already more diffuse compared to the chlorite case. Furthermore, below the solute the density is now shifted to the space between the chlorate oxygen atoms, Figure 6b. This tendency is continued in case of perchlorate, where the spatial density is now dominantly shifted to the volume between the oxygen atoms, Figure 6c.

Structure of the hypochlorite ion in aqueous solution

The experimental RDF from the LAXS measurement of the aqueous solution of sodium hypochlorite is significantly different from the oxo chloro anions with in general weak contributions and with peaks at ca. 1.0, 1.6, 3.25 and 4.6 Å and shoulders at 2.4 and 3.9 Å, Figure S4†. The weak peak at 1.6 Å corresponds to the Cl-O bond distance, and the shoulder at 3.9 Å to the $\text{Cl}(-\text{O})\cdots\text{O}_{\text{aq}}$ distance. The main contributions to the strong peak at 3.25 Å are from $\text{Cl}\cdots(\text{H}-)\text{O}_{\text{aq}}$ distances and the mean $\text{O}_{\text{aq}}\cdots\text{O}_{\text{aq}}$ distance in the aqueous bulk. However, the latter distance is much longer and weaker than found in the other aqueous solutions in this and other studies. One may therefore regard this solution as a kind melt of hydrated ions even though the excess of water should be enough to form an aqueous solution. The hypochlorite ion binds ca. five water molecules through hydrogen bonds to the chlorine atom molecules at the same distance, 3.25 Å, as the chloride ion which binds six water molecules.^{54,55} The observed Cl-O bond distance is in the expected region, 1.66 Å, even though no compounds with a hypochlorite ion have been characterised in the solid state so far. This oxo oxygen binds ca. three water molecules through hydrogen bonds concluded from the observed $\text{Cl}(-\text{O})\cdots\text{O}_{\text{aq}}$ distance, 3.85 Å corresponding to a tetrahedral configuration around the hypochlorite oxygen. The structure of the hydrated sodium ion was modelled as a regular octahedron with a mean Na-O bond distances of 2.42(2) Å in full agreement with previous studies.⁵⁰ The experimental and calculated RDFs, and the refined intensity function using the parameters given in Table 2 are shown in Figure S4† together with the individual contributions from the hydrated hypochlorite and sodium ions, and the aqueous bulk.

Structure of the bromate, iodate and metaperiodate ions in aqueous solution

The experimental RDFs from the LAXS measurement of the aqueous solutions of sodium bromate, iodate and metaperiodate show the same pattern of peaks as the chlorate and perchlorate ions, Figures S5-S7†. The weak peak at 1.6, 1.85 and 1.8 Å corresponds to the X-O bond distance, and the peak at 4.05, 4.3 and 4.25 Å to the X(-O)…O_{aq} distance, respectively. The refined distances are given in Table 2. The Br-O and I-O bond distances in selected anhydrous bromate, iodate and metaperiodate and orthoperiodate salts are given in Table S1† for comparison. The major difference between the bromo and iodo analogues from the chloro ones in aqueous solution is that the X(-O)…O_{aq} distance is longer and corresponds to a triangular configuration around the bromate, iodate and metaperiodate oxygens, strongly indicating that only two water molecules are hydrogen bonded. However, this is in accordance with previous studies of oxo anions with central atoms from the fourth and fifth series including the arsenite, arsenate, selenite, selenate ions and telluric acid.^{56,57} The structure of the hydrated sodium ion was modelled as a regular octahedron with a mean Na-O bond distance of 2.43 Å.⁵⁰ The experimental and the calculated RDFs and the refined intensity functions using the parameters given in Table 2 are shown in Figures S5-S7† together with the individual contributions from the hydrated bromate, iodate, metaperiodate and sodium ions, and the aqueous bulk.

The bromate ion has also been studied by EXAFS in the solid state, as the sodium salt, and in aqueous solution. The Br-O bond distance in aqueous solution as determined by EXAFS is 1.654(2) Å, which is in excellent agreement with the result obtained by LAXS, Tables 2 and 6. An EXAFS study of solid sodium bromate gave a Br-O bond distance of 1.646 Å, which is in excellent agreement with XRD studies.^{58,59}

EXAFS study of sodium metaperiodate and orthoperiodate in solid state and aqueous solution

Periodate is present in two forms, meta and ortho. In metaperiodate iodine binds to four oxygens in regular tetrahedron with a mean I-O bond distance of 1.756 Å, Table S1†, and with a narrow bond distance distribution. Iodine binds to six oxygens in orthoperiodate with a mean I-O bond distance of 1.886 Å, Table S1†, and with a quite broad bond distance distribution. EXAFS

data on solid sodium meta- and orthoperiodate confirm these observations, Table 7. However, EXAFS data on aqueous solutions of sodium meta- and orthoperiodate show a different picture, with an I-O bond distance of 1.78 Å independent of periodate source showing clearly that metaperiodate is the dominating form in aqueous solution, Table 6, Figures S8 and S9†.

Impact of structural symmetry and lone electron-pairs on the hydration of oxo anions

The first study in this series of hydration of oxo anions in aqueous solution on the sulfate ion showed that the three hydrating water molecules on each sulfate oxygen exchange directly with water molecules in the surrounding bulk, Figures 7 middle right and S10 right panel†.⁸ The (S-)O···H-O hydrogen bond is somewhat stronger and shorter than the H-O···H-O hydrogen bond in pure water, and the MRT of 2.6 ps^{8,19} is longer than in pure water 1.7 ps,¹⁸ clearly demonstrating that the sulfate ion can be regarded as a structure making ion. The perchlorate ion has several similarities with the sulfate ion as it has tetrahedral symmetry, three water molecules are hydrogen bonded to each perchlorate oxygen, and there is a direct water exchange with the surrounding bulk water, Figures 7 lower left and S10 left panel†. However, due to the lower charge density of the perchlorate ion the respective hydrogen bonds are weaker than those in pure water,¹⁹ and the MRT is shorter, 1.4 ps. The third highly symmetric oxo anion studied is the selenate ion.⁵⁶ However, for the selenate ion only the structure and hydrogen bond strength studies have been performed. The hydrated selenate ion display the expected similarities with the sulfate ion, with shorter and stronger hydrogen bonds to the hydrating water molecules than in pure water, and it can be assumed that also the selenate ion exchanges the hydrating water molecules directly with water bulk. On the other hand, there is one surprising difference between sulfate and perchlorate on one hand, and selenate,⁵⁶ selenite,⁵⁶ bromate, iodate, periodate and arsenate⁵⁷ ions on the other, namely, that only two water molecules hydrogen bind to the oxygens of the latter. Its seems to be systematic that oxo anions of elements in the third series in the periodic table, independent of oxidation state of the central atom,

three water molecules are hydrogen bonded to each oxygen, while those in the fourth or higher series bind only two. The reason for this behaviour is not yet understood.

The thiosulfate ion has lower structural symmetry than sulfate due to the presence of the sulfur atom in the fourth vertex.⁹ It is expected that the hydration of the sulfur is weaker than of the oxygen atoms due to its lower charge density, but otherwise the hydration properties of the sulfate and thiosulfate ions should be similar. This is indeed also observed in both QMCF/MD simulations and experimental studies. The mean hydrogen bond lifetimes to the oxygens and the terminal sulfur atom in thiosulfate are 2.25 and 1.16 ps,⁹ respectively, showing that the S···H(-OH) hydrogen bond is indeed much more weaker and labile than the O···H(-OH) ones.⁹ For both the oxygens and the sulfur, the hydrating water molecules are directly exchanged with bulk water molecules, Figure 7 lower right. From this point of view the thiosulfate ion behaves mechanistically as a symmetric anion even though it has lower symmetry than the sulfate ion.⁸ As the strength and the water exchange rate of the hydrogen bonds to the oxygens and the sulfur atom differ significantly with former stronger and the latter weaker than the hydrogen bonds in pure water, thus, the oxygen side of the thiosulfate ion acts as a structure maker while the sulfur vertex as a structure breaker.

The sulfite, chlorate and chlorite ions have one or two lone electron-pairs and thereby lower symmetry than the sulfate and perchlorate ions, which seem to affect the hydration properties significantly. The sulfite ion, being a structure maker, does not exchange water molecules directly with bulk water as the sulfate and thiosulfate ions do. Instead the hydrating water molecules are transported to the lone electron-pair region where it is exchanged with bulk water, Figure 7 upper right.¹⁰ This is a complex water exchange mechanism which extend the lifetime of these water molecules compared to direct exchange. Therefore, the MRT for the sulfite ion is not comparable with the MRT values given above for the sulfate, perchlorate and thiosulfate ions, Table 5. One of the main points in the present study is to determine whether the chlorate and chlorite ions, with one and two lone electron-pairs, respectively, have the same kind mechanistic water exchange behaviour as the sulfite ion. An important difference is that the chlorate and chlorite ions are

structure breakers and thereby the hydrogen bonds to the oxygen atoms are proportionately weaker. This makes the spatial occupancy less well-defined than for the sulfite ion and it turned out that it is not possible to follow any well-defined migration pattern, as it is difficult to distinguish between hydrated and bulk water in the region close to these ions. Fitting of the hydrogen bond correlation functions gave hydrogen bond lifetimes for $O \cdots H-O_{aq}$ for the chlorite, chlorate and perchlorate ions of 0.42, 0.16 and 0.14 ps, respectively. This shows that the hydrogen bond lifetime is about the same for the chlorate and perchlorate ions, and that the lone electron-pair on the chlorate ion has limited impact on the water exchange mechanism, which seems similar to the perchlorate ion, Figure 7 middle left. On the other hand, the hydrogen bond lifetime of the hydrating water molecules on the chlorite ion is almost three times as long as for the chlorate and perchlorate ions, Table 5. The hydrogen bonds to chlorite are not stronger, and instead there may be a kinetic component which is not fully understood. It is likely that the chlorite ion has a complex water exchange mechanism, as the hydrogen bond lifetime is surprisingly long, but as the hydrating water molecules are weakly bonded, the migration pattern is less well-defined, Figure 7 upper left, compared to the sulfite ion, Figure 7 middle right, and any detailed conclusions about the water exchange mechanism cannot be made.

The major factors deciding the water exchange mechanism on oxo anions seem to be the hydrogen bond strength, whether the ion is a structure maker or breaker is largely determined by the total charge of the ion and if there is a lone electron-pair or not. For oxo anions with high symmetry and no lone electron-pairs a simple water exchange between the hydrating water molecules and the aqueous bulk takes place. Replacing an oxygen atom for a sulfur one, as in the thiosulfate ion, does not appear to affect the water exchange mechanism even though the exchange rate on the oxygen and the sulfur atoms differ significantly. For the weakly hydrated monovalent oxo anions the hydrating water molecules move almost as freely as bulk water and it is difficult to track any well-defined migration patterns. The structure making sulfite ion with a lone electron-pair displays a complex water exchanging mechanism with transport within the hydration shell region before

exchange in close vicinity to the lone electron-pair.

Conclusions

LAXS measurements on the hydrated chlorite, ClO_2^- , chlorate, ClO_3^- , perchlorate ClO_4^- , bromate, BrO_3^- , iodate, IO_3^- and metaperiodate, IO_4^- , ions show that water molecules are weakly hydrogen bonded to the oxygens, and that the oxygens of the oxo chloro anions bind three water molecules each, while bromate, iodate and periodate oxygens bind only two water molecules. It has not been possible to determine any distance to the water molecules which most likely are clustered outside the lone electron-pair of the chlorite, chlorate, bromate and iodate ions as was for the structure making sulfite ion.⁹ The mean X-O bond distance of the oxo halo anions is 0.01-0.02 Å longer in water than in anhydrous salts in solid state, see Tables 2 and 6. The LAXS study of the hypochlorite ion, ClO^- , shows a different hydration pattern with large similarities with the hydrated chloride ion. In the hydrated hypochlorite ion the Cl-O bond distance is 1.66(2) Å, five water molecules are hydrogen bonded to chlorine at a $\text{Cl}\cdots(\text{H})\text{-O}$ distance of 3.25(1) Å, and the hypochlorite oxygen binds three water molecules. For comparison, the chloride ion forms six hydrogen bonds to the hydrating water molecules at 3.25 Å.^{50,55} An EXAFS study of solid and aqueous solution of sodium orthodihydrogenperiodate, $\text{Na}_3\text{H}_2\text{IO}_6$, show that the predominant form of periodate present in aqueous solution is best represented as hydrated metaperiodate, IO_4^- . The hydration of the monovalent oxo halo anions is much weaker than on the divalent oxo sulfur and seleno anions. The difference in ordering of water molecules between structure making and breaking ions is clearly seen in Figure 7. The oxosulfur anions display a well-defined valley between the hydration shell and the bulk (deep blue in Figures 7 and S10), while for oxo halo anions this valley is shallow showing that it is difficult to distinguish between hydrating and bulk water (light blue in Figures 7 and S10), and thereby it is not possible to follow any well-defined migration pattern. The Cl-O bond distances in the hydrated oxo chloro anions obtained in the

QMCF MD simulations are in excellent agreement with experimentally determined by LAXS. The mean residence time for the perchlorate ion is significantly shorter, $\tau_{0.5}=1.4$ ps, compared to the sulfate ion and pure water, $\tau_{0.5}=2.6$ and 1.7 ps, respectively. The angular radial distribution functions show that the chlorate ion behave similar to the perchlorate ion with a fast water exchange at the oxygens while the chlorite ion has a more complex mechanism with a significantly slower exchange rate.

Acknowledgments

We gratefully acknowledge the financial support from the Swedish Research Council and the Austrian Science Foundation. This work was supported by the Austrian Ministry of Science “BMWF UniInfrastrukturprogramm” as part of the Research Focal Point Scientific Computing at the University of Innsbruck. Part of this research has been performed at the Stanford Synchrotron Radiation Light-source, SLAC National Accelerator Laboratory, which is supported by the U.S. Department of Energy, Office of Science, Office of Basic Energy Sciences under Contract No. DE-AC02-76SF00515. The SSRL Structural Molecular Biology Program is supported by the DOE Office of Biological and Environmental Research, and by the National Institutes of Health, National Institute of General Medical Sciences (including P41GM103393). The contents of this publication are solely the responsibility of the authors and do not necessarily represent the official views of NIGMS or NIH.

References

- 1 I. Persson, *Pure Appl. Chem.* 2010, **82**, 1901-1917.
- 2 L. Helm and A. E. Merbach, *Coord. Chem. Rev.* 1999, **187**, 151-181.
- 3 J. Stangret and T. Gampe, *J. Phys. Chem. A* 2002, **106**, 5393-5402.
- 4 B. M. Rode, C. F. Schwenk, T. S. Hofer and B. R. Randolph, *Coord. Chem. Rev.*, 2005, **249**, 2993-3006.
- 5 B. M. Rode, T. S. Hofer, A. B. Pribil and B. R. Randolph, *Theoretical and Computational Inorganic Chemistry*, Eds. R. van Eldik and J. Harvey, ISBN 978-0-12-380874-5, Elsevier, Amsterdam 2010.
- 6 A. K. H. Weiss and T. S. Hofer, *RSC Adv.*, 2013, **3**, 1606-1635.
- 7 A. Tongraar, S. Hannongbua, B. M. Rode, *J. Phys. Chem. A* 2010, **114**, 4334-4339.
- 8 V. Vchirawongkwin, B. M. Rode and I. Persson, *J. Phys. Chem. B* 2007, **111**, 4150-4155.
- 9 L. Eklund, T. S. Hofer, A. Pribil, B. M. Rode and I. Persson, *Dalton Trans.* 2012, **41**, 5209-5216.
- 10 L. Eklund, T. S. Hofer, A. K. H. Weiss, A. O. Tirler, and I. Persson, *Dalton Trans.* 2014, **43**, 12711-12720.
- 11 T. Sakwarathorn, S. Pongstabodee, V. Vchirawongkwin, L. R. Canaval, A. O. Tirler and T. S. Hofer, *Chem. Phys. Lett.* 2014, **595-596**, 226-229.
- 12 E. Hinteregger, A. B. Pribil, T. S. Hofer, B. R. Randolph, A. K. H. Weiss and B. M. Rode, *Inorg. Chem.* 2010, **49**, 7964-7968.
- 13 I. Persson, M. Sandström, H. Yokoyama and M. Chaudhry, *Z. Naturforsch., Sect. A* 1995, **50**, 21-37.
- 14 T. S. Hofer, H. T. Tran, C. F. Schwenk and B. M. Rode, *J. Comput. Chem.*, **2004**, *25*, 211-217.
- 15 N. N. Greenwood and A. Earnshaw, *Chemistry of the Elements*, 2nd edition, Elsevier, Oxford, UK, 1997.
- 16 *The IUPAC Stability Constants Database*, Academic Software, Sourby Old Farm, Ottley, UK.
- 17 A. T. Winfree, *J. Chem. Educ.*, 1984, **61**, 661-663.
- 18 L. Malaprade, *Bull. Soc. Chim. Fr.*, **1934**, *3*, 833.
- 19 J. and T. Gampe, *J. Phys. Chem. A*, 2002, **106**, 5393-5402, and references therein.
- 20 I. Persson, K. Lyczko, D. Lundberg, L. Eriksson, and A. Płaczek, *Inorg. Chem.*, 2011, **50**, 1058-1072.
- 21 C. M. V. Stålhandske, I. Persson, M. Sandström and E. Kamienska-Piotrowicz, *Inorg. Chem.*, 1997, **36**, 3174-3182.
- 22 G. Johansson and M. Sandström, *Chem. Scr.*, 1973, **4**, 195-198.
- 23 M. Molund and I. Persson, *Chem. Scr.*, 1985, **25**, 197-197.

- 24 J. P. Chandler, *Behav. Sci.*, 1969, **14**, 81-82.
- 25 A. J. C. Wilson, Ed. *International Tables for Crystallography*; Kluwer Academic Publishers: Dordrecht, The Netherlands, 1995; Vol. C.
- 26 D. T. Cromer, *J. Chem. Phys.*, 1967, **47**, 1892-1893.
- 27 D. T. Cromer, *J. Chem. Phys.*, 1969, **50**, 4857-4859.
- 28 A. Thompson, D. Attwood, E. Gullikson, M. Howells, K.-J. Kim, J. Kirz, J. Kortright, I. Lindau, Y. Liu, P. Pianetta, A. Robinson, J. Scofield, J. Underwood, G. Williams and H. Winick, *H. X-ray data booklet*; Lawrence Berkley National Laboratory, 2009.
- 29 G. N. George and I. J. Pickering, *EXAFSPAK - A suite of Computer Programs for Analysis of X-ray absorption spectra*; SSRL: Stanford, CA.
- 30 S. I. Zabinsky, J. J. Rehr, A. Ankudinov, R. C. Albers and M. J. Eller, *Phys. Rev. B*, 1995, **52**, 2995-3009.
- 31 A. Warshel and M. Levitt, *J. Mol. Biol.*, 1976, **103**, 227-249.
- 32 M. J. Field, P. A. Bash, and M. Karplus, *J. Comp. Chem.*, 1990, **11**, 700-733.
- 33 J. Gao, *J. Am. Chem. Soc.*, 1993, **115**, 2930-2935.
- 34 D. Bakowies and W. Thiel, *J. Phys. Chem.*, 1996, **100**, 10580-10594.
- 35 M. Svensson, S. Humbel, R. D. J. Froese, T. Matsubara, S. Sieber, and K. Morokuma, *J. Phys. Chem.*, 1996, **100**, 19357-19363.
- 36 H. M. Senn and W. Thiel, *Curr. Opin. Chem. Biology*, 2007, **11**, 182-187.
- 37 H. Lin and D. G. Truhlar, *Theor. Chim. Acta*, 2007, **117**, 185-199.
- 38 B. M. Rode, T. S. Hofer, B. R. Randolph, C. F. Schwenk, D. Xenides and V. Vchirawongkwin, *Theor. Chim. Acta*, 2006, **115**, 77-85.
- 39 T. S. Hofer, A. B. Pribil, B. R. Randolph and B. M. Rode, *Adv. Quant. Chem.*, 2010, **59**, 213-246.
- 40 T. S. Hofer, B. M. Rode, A. B. Pribil and B. R. Randolph, *Adv. Inorg. Chem.*, 2010, **62**, 143-175.
- 41 H. J. C. Berendsen, J. P. M. Postma, W. F. van Gunsteren, A. DiNola and J. R. Haak, *J. Chem. Phys.* 1984, **81**, 3684-3690.
- 42 H. J. C. Berendsen, J. R. Grigera and T. P. Straatsma, *J. Phys. Chem.*, 1987, **91**, 6269-6271.
- 43 M. P. Allen and D. J. Tildesley, *Computer Simulation of Liquids*, Oxford Science Publications, Oxford, 1990.
- 44 T. H. Dunning, *J. Chem. Phys.*, 1970, **53**, 2823-2833.
- 45 E. Magnusson and H. F. Schaefer, *J. Chem. Phys.*, 1985, **83**, 5721-5726.
- 46 R. Ahlrichs, M. Bär, M. Häser, H. Horn and C. Kölmel, *Chem. Phys. Lett.*, 1989, **162**, 165-169.
- 47 F. H. Stillinger and A. Rahman, *J. Chem. Phys.*, 1978, **68**, 666-670.
- 48 P. Bopp, G.; Jansco and K. Heinzinger, *Chem. Phys. Lett.*, 1983, **98**, 129-133.

- 49 W. Humphrey, A. Dalke and K. Schulten, *J. Mol. Graph.*, 1996, **14**, 33-38.
- 50 J. Mähler and I. Persson, *Inorg. Chem.*, 2012, **51**, 425-438.
- 51 F. H. Allen, *Acta Crystallogr., Sect. B: Struct. Sci.*, 2002, **58**, 380-388.
- 52 *Inorganic Crystal Structure Database*, National Institute of Standards and Technology and FIZ, Karlsruhe, release 2013/2.
- 53 A. B. Pribil, T. S. Hofer, B. R. Randolph and B. M. Rode, *J. Comput. Chem.* 2008, **29**, 2330-2334.
- 54 F. Jalilehvand, D. Spångberg, P. Lindqvist-Reis, K. Hermansson, I. Persson and M Sandström, *J. Am. Chem. Soc.* 2001, **123**, 431-441.
- 55 H. Ohtaki and T. Radnai, *Chem. Rev.* 1993, **93**, 1157-1204, and references therein.
- 56 L. Eklund and I. Persson, *Dalton Trans.*, 2014, **43**, 6315-6321.
- 57 J. Mähler and I. Persson, *Dalton Trans.*, 2013, **42**, 1364-1377.
- 58 S. C. Abrahams and J. L. Bernstein, *Acta Crystallogr., Sect. B*, 1977, **33**, 3601-3604.
- 59 D. H. Templeton and L. K. Templeton, *Acta Crystallogr., Sect. A*, 1985, **41**, 133-142.

Table 1. Concentrations of all ions and water in mol·dm⁻³ of the solutions studied by LAXS (*L*) and EXAFS (*E*), including their densities, ρ , and linear absorption coefficient μ

Sample	[X-]	[Na ⁺]	[H ₃ O ⁺]	[H ₂ O]	$\rho/\text{g}\cdot\text{cm}^{-3}$	μ/cm^{-1}	Method
NaClO	2.430	2.430		56.902	1.2060	2.449	<i>L</i>
NaClO ₂	2.0060	2.0060		51.351	1.1065	2.158	<i>L</i>
NaClO ₃	2.0177	2.0177		52.030	1.1521	2.222	<i>L</i>
HClO ₄	2.0014		2.0014	49.996	1.1107	2.064	<i>L</i>
NaBrO ₃	1.5530	1.5530		54.502	1.2162	10.420	<i>L</i>
NaIO ₃	0.4548	0.4548		55.168	1.0839	3.402	<i>L</i>
NaIO ₄	0.6751	0.6751		53.560	1.1904	4.449	<i>L</i>
NaBrO ₃	0.50	0.50					<i>E</i>
NaIO ₄	0.50	0.50					<i>E</i>
Na ₃ H ₂ IO ₆	0.20	0.60					<i>E</i>

Table 2. Mean bond distances, $d/\text{\AA}$, number of distances, N , temperature coefficients, $b/\text{\AA}^2$, and the root-mean-square variation (hwhh), $l/\text{\AA}$, in the LAXS studies of the aqueous sodium hypochlorite, chlorite, chlorate, bromate, iodate and periodate, and perchloric acid solutions at room temperature, and from the QMCF MD simulation of the chlorite, chlorate and perchlorate ions in aqueous solution.

Interaction	N	d	b	l	d	l
LAXS						QMCF MD
<i>Hypochlorite ion, ClO^-</i>						
Cl-O	1	1.662(6)	0.0058(8)	0.108(7)		
Cl...O _{aq}	5	3.251(5)	0.0127(5)	0.159(4)		
Cl(-O)...O _{aq}	3	3.85(2)	0.022(2)	0.21(1)		
O...O _{aq} /O _{aq} ...O _{aq}	2	3.045(8)	0.025(2)	0.22(1)		
Na-O _{aq}	6	2.422(9)	0.0283(7)	0.24(1)		
<i>Chlorite ion, ClO_2^-</i>						
Cl-O	2	1.591(3)	0.0045(4)	0.069(7)	1.576(6)	0.067(1)
Cl...O _{aq}	6	3.881(6)	0.031(1)	0.25(1)	3.783(2)	0.92(4)
O...O _{aq}	2	3.045(8)	0.025(2)	0.23(1)	2.7875	0.454(2)
Na-O _{aq}	6	2.428(8)	0.0244(7)	0.221(3)		
O _{aq} ...O _{aq}	2	2.890(2)	0.0210(3)	0.205(2)		
<i>Chlorate ion, ClO_3^-</i>						
Cl-O	3	1.501(2)	0.0030(4)	0.077(5)	1.487(0)	0.058(7)
Cl...O _{aq}	9	3.770(6)	0.0187(4)	0.193(3)	3.960(3)	0.93(1)
O...O _{aq}	2	3.021(4)	0.0251(6)	0.224(3)	2.9252(8)	0.75(5)
Na-O _{aq}	6	2.434(6)	0.0233(5)	0.216(3)		
O _{aq} ...O _{aq}	2	2.889(2)	0.0198(3)	0.199(2)		
<i>Perchlorate ion, ClO_4^-</i>						
Cl-O	4	1.453(2)	0.0020(2)	0.063(3)	1.447(6)	0.064(0)
Cl...O _{aq}	12	3.757(6)	0.0306(9)	0.247(4)	4.076(3)	0.69(2)
O...O _{aq}	2	3.046(7)	0.0234(5)	0.216(3)	3.151(3)	0.70(4)
(H-)O...O _{aq}	4	2.693(6)	0.0109(5)	0.148(3)		
O _{aq} ...O _{aq}	2	2.890(2)	0.0186(2)	0.192(2)		
<i>Bromate ion, BrO_3^-</i>						
Br-O	3	1.671(2)	0.0020(2)	0.063(6)		
Br...O _{aq}	9	4.068(6)	0.0282(7)	0.237(3)		
O...O _{aq}	2	2.987(8)	0.0257(6)	0.227(3)		
Na-O _{aq}	6	2.434(6)	0.0233(5)	0.216(3)		
O _{aq} ...O _{aq}	2	2.890(2)	0.0200(3)	0.200(2)		
<i>Iodate ion, IO_3^-</i>						
I-O	3	1.829(5)	0.0056(4)	0.106(4)		
I...O _{aq}	9	4.27(1)	0.0187(4)	0.193(3)		
O...O _{aq}	2	3.013(4)	0.0258(6)	0.224(3)		
Na-O _{aq}	6	2.432(6)	0.0251(5)	0.216(3)		

$O_{aq} \cdots O_{aq}$	2	2.890(2)	0.0200(2)	0.200(2)
<i>Metaperiodate ion, IO_4^-</i>				
I-O	4	1.781(2)	0.0061(2)	0.110(3)
I- $\cdots O_{aq}$	12	4.243(4)	0.0259(6)	0.228(2)
$O \cdots O_{aq}$	2	3.009(4)	0.0268(8)	0.232(3)
Na-O _{aq}	6	2.43(2)	0.029(3)	0.24(2)
$O_{aq} \cdots O_{aq}$	2	2.890(2)	0.0199(2)	0.200(2)

Table 3. Continuous hydrogen bond correlation function $S_{HB}(t)$ fitted to $S_{HB}(\tau) = a_0 e^{-t/\tau_1} + (1-a_0) e^{-t/\tau_2}$, ld indicates linear dependence of the parameters essentially transforming the fit to a single exponential decay.

Interaction	a_0	τ_1	τ_2
<chem>ClO2^-</chem>			
O _A ···H-O _{aq}	0.455	0.136	0.471
O _B ···H-O _{aq}	0.059	0.0194	0.360
Cl···H-O _{aq}	0.530	0.0383	0.239
<chem>ClO3^-</chem>			
O _A ···H-O _{aq}	0.360	0.0372	0.145
O _B ···H-O _{aq}	0.138	0.0320	0.177
O _C ···H-O _{aq}	0.996	0.129	ld
Cl···H-O _{aq}	0.986	0.107	ld
<chem>ClO4^-</chem>			
O _A ···H-O _{aq}	0.517	0.0124	0.0881
O _B ···H-O _{aq}	0.257	0.0293	0.130
O _C ···H-O _{aq}	0.243	0.0465	0.123
O _D ···H-O _{aq}	0.523	0.0523	0.217

Table 4. Atomically centered mean residence times, MRTs, and average number of exchanges required to achieve one lasting exchange longer than 0.5 ps, R_{ex} , of water molecules in the hydrated thiosulfate from simulations on HF theory level

Atom	$t^*=0.0 \text{ ps}$		$t^*=0.5 \text{ ps}$		
	MRT	$N_{\text{ex}}/10\text{ps}$	MRT	$N_{\text{ex}}/10\text{ps}$	R_{ex}
<i>Chlorite</i>					
Cl	257		1.6	76	3.4
O	170		1.7	36	4.7
O	142		2.2	27	5.3
<i>Chlorate</i>					
Cl	234		2.1	67	3.5
O	251		1.1	46	5.5
O	229		1.2	40	5.7
O	252		1.2	41	6.2
<i>Perchlorate</i>					
O	408		1.02	49	8.3
O	429		0.84	54	7.9
O	373		0.98	49	7.6
O	382		0.92	54	7.1

Table 5. Mean residence times, MRTs, $\tau_{0.5}$, and the sustainability coefficients, S_{ex} , of water molecules in the hydrated chlorite, chlorate, perchlorate, thiosulfate, sulfite, sulfate and phosphate ion and bulk water from simulations on HF theory level.

Hydrated ion	$\tau_{0.5}$	$N_{\text{ex}}^{0.5}$	$N_{\text{ex}}^{0.0}$	$1/S_{\text{ex}}$	Reference
Perchlorate	1.4	106	431	4.1	a
Sulfate	2.6	54	399	7.4	5
Phosphate	3.9	42	132	3.1	44
Chlorate	2.1	67	234	3.5	a
Sulfite	3.2	59	346	5.9	7
Chlorite	1.6	76	257	3.4	a
Bulk water	1.7	24	269	11.2	8

^a This work

Table 6. Mean bond distances, $d/\text{\AA}$, number of distances, N , and Debye-Waller coefficients, $\sigma^2/\text{\AA}^2$, in the EXAFS study of solid sodium bromate, NaBrO_3 , sodium metaperiodate, NaIO_4 , solid sodium orthoperiodate, $\text{Na}_3\text{H}_2\text{IO}_6$, and aqueous solutions of these salts at room temperature. The refinements were performed in the k range $2\text{-}13 \text{\AA}^{-1}$. $F/\%$ is the goodness of fit as defined in the EXAFSPAK program.

Species	Interaction	N	d	σ^2	F
<i>Solid NaBrO₃</i>					
BrO_3^-	Br-O	4	1.650(1)	0.0013(1)	7.9
	Br···Br	1	4.149(5)	0.0095(4)	
<i>0.50 mol·dm⁻³ NaBrO₃ in water</i>					
BrO_3^-	Br-O	4	1.662(1)	0.0014(1)	7.8
	MS (BrO ₃)	6	3.000(9)	0.0065(8)	
	MS (BrO ₃)	3+6	3.33(2)	0.005(2)	
<i>Solid NaIO₄</i>					
IO_4^-	I-O	4	1.770(1)	0.0013(1)	7.9
	I···I	1	4.010(5)	0.0095(4)	
<i>0.50 mol·dm⁻³ NaIO₄ in water</i>					
IO_4^-	I-O	4	1.778(1)	0.0014(1)	7.8
	MS (IO ₄)	12	3.20(1)	0.005(2)	
<i>Solid Na₃H₂IO₆</i>					
$\text{H}_3\text{IO}_6^{2-}$	I-O	6	1.866(1)	0.0046(1)	8.5
	MS (IO ₆)	3x6	3.76(2)	0.008(2)	
<i>Saturated Na₃H₂IO₆ in water</i>					
IO_4^-	I-O	4	1.782(1)	0.0018(1)	7.3
	MS (IO ₄)	12	3.22(2)	0.005(2)	

Table 7. Comparison of I-O bond distances in \AA of metaperiodate and orthoperiodate ions in solid state and aqueous solution.

Method	$\text{NaIO}_4(\text{s})$	$\text{Na}_3\text{H}_2\text{IO}_6(\text{s})$	NaIO_4 in water	$\text{Na}_3\text{H}_2\text{IO}_6$ in water
XRD	1.769	1.912		
EXAFS	1.770	1.866	1.778	1.782
LAXS			1.781	

Legends to Figures

Figure 1. Structure and mean life time of the hydrogen bonds between the oxygen and sulfur atoms and the hydrating water molecules of the hydrated sulfite (left), sulfate (middle) and thiosulfate ions (right) in aqueous solution obtained from previous LAXS and simulation studies, refs. 6-8.

Figure 2. LAXS, chlorate ion. Top: the individual peak shapes for all contributing species in the $1.5006 \text{ mol}\cdot\text{dm}^{-3}$ aqueous solution of sodium chlorate, the hydrated chlorate ion (orange line), hydrated sodium ion (brown line) and the aqueous bulk (green line). (b) Experimental $D(r) - 4\pi r^2 \rho_0$ (red line); model (black line), the modelled distances are given in Table 2; difference (blue line). Bottom: reduced LAXS intensity function, $si_{\text{exp}}(s)$ (thin black line); model $si_{\text{calc}}(s)$ (red line).

Figure 3. Angular radial distribution function, showing the chlorite (left), chlorate (middle) and perchlorate (right) using 18° overlapping radial cones and a 1000×1000 interpolation grid. A substantial deviation from symmetric hydration shell can be observed in chlorite and chlorate while the perchlorate shows a minimum at a symmetric distance from the oxygens.

Figure 4. Continuous hydrogen bond correlation function $S(t)$ for chlorite (top), chlorate (middle) and perchlorate (bottom), red solid line depicts $\text{Cl}\cdots\text{H}-\text{O}$ bond, black solid line $\text{O}\cdots\text{H}-\text{O}$ bond. The dashed lines are the corresponding fitted curves.

Figure 5. Coordination number distribution of a) chlorite, b) chlorate and c) perchlorate obtained from the QMCF MD simulations. The corresponding average coordination numbers are 9.8, 11.1 and 12.0, respectively.

Figure 6. Snapshots (left) and spatial oxygen density (right) obtained from QMCF MD simulations of a) chlorite, b) chlorate and c) perchlorate in aqueous solution.

Figure 7. Angular radial distribution functions for the ions in this study compared with ions in earlier work. All the studied ions show a well distributed low occupancy around the shell, typical for structure breakers when compared with the ions of the previous work which show much stronger signals in $G_{X\cdots O}(r,\alpha)$ typical for structure makers. Left column from top: ClO_2^- , ClO_3^- , ClO_4^- ; right column from top: SO_3^{2-} , SO_4^{2-} , $\text{S}_2\text{O}_3^{2-}$.

Figure 1

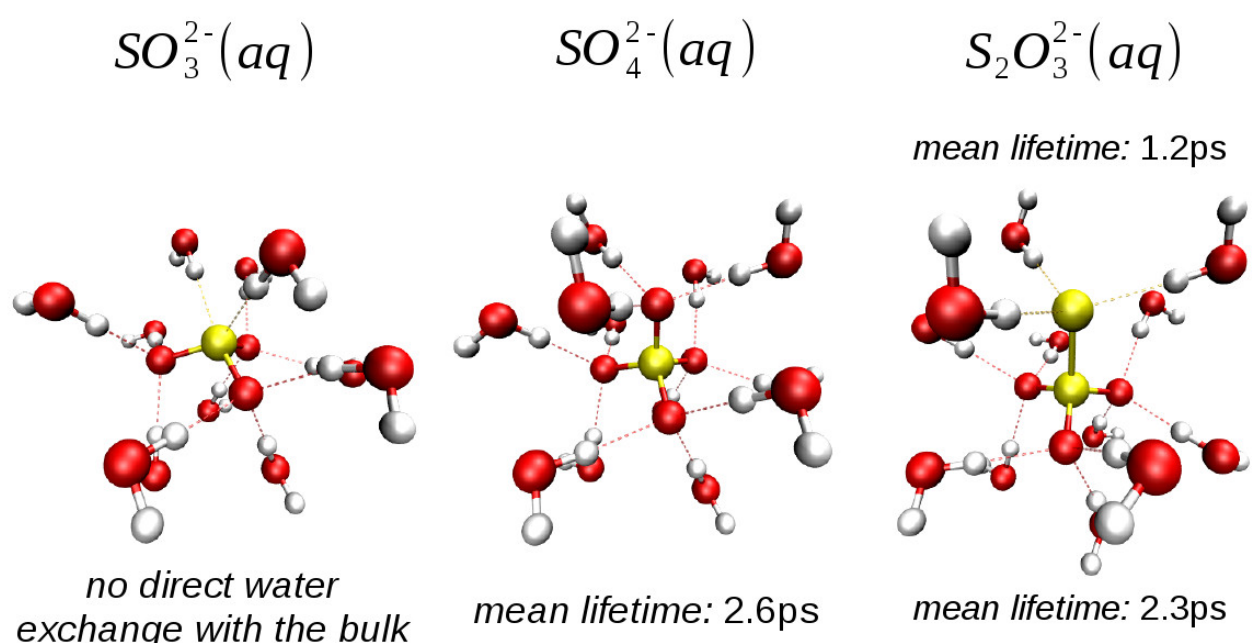


Figure 2

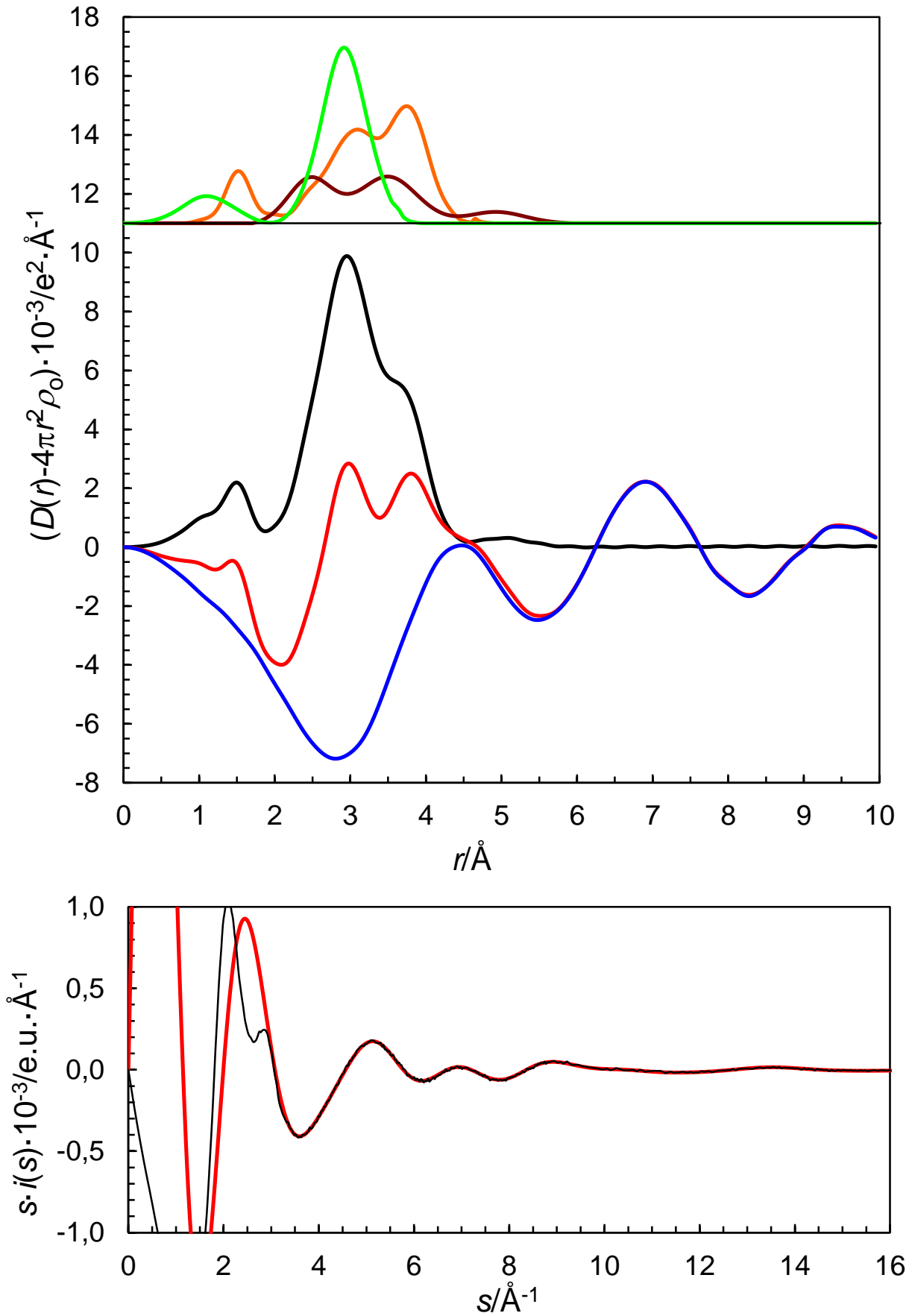


Figure 3

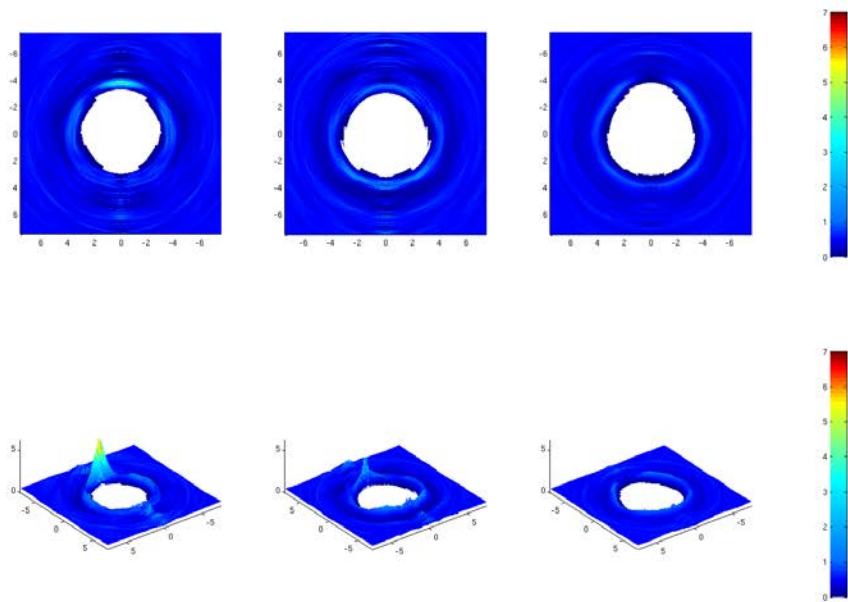


Figure 4

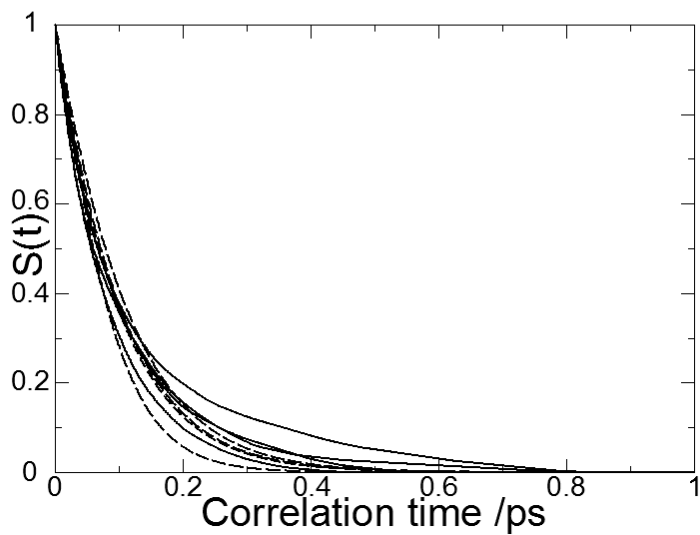
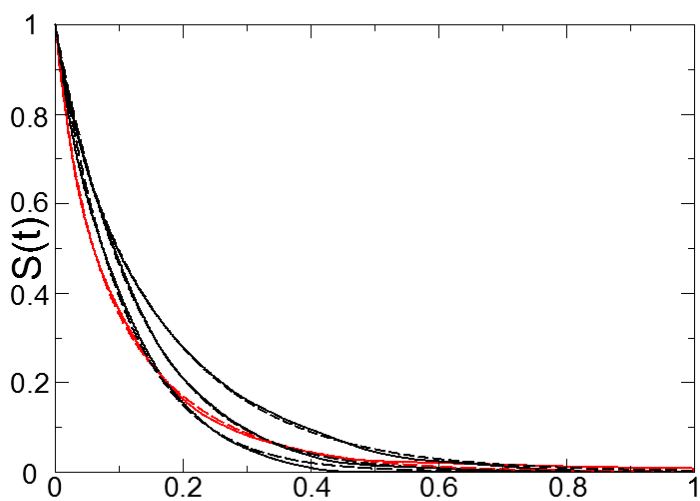
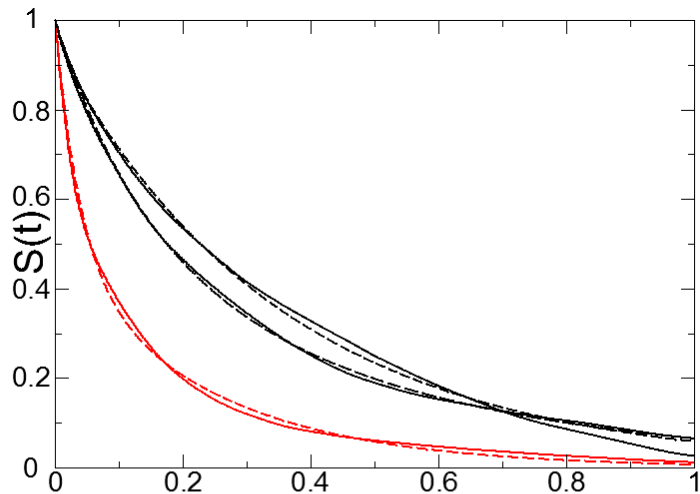


Figure 5

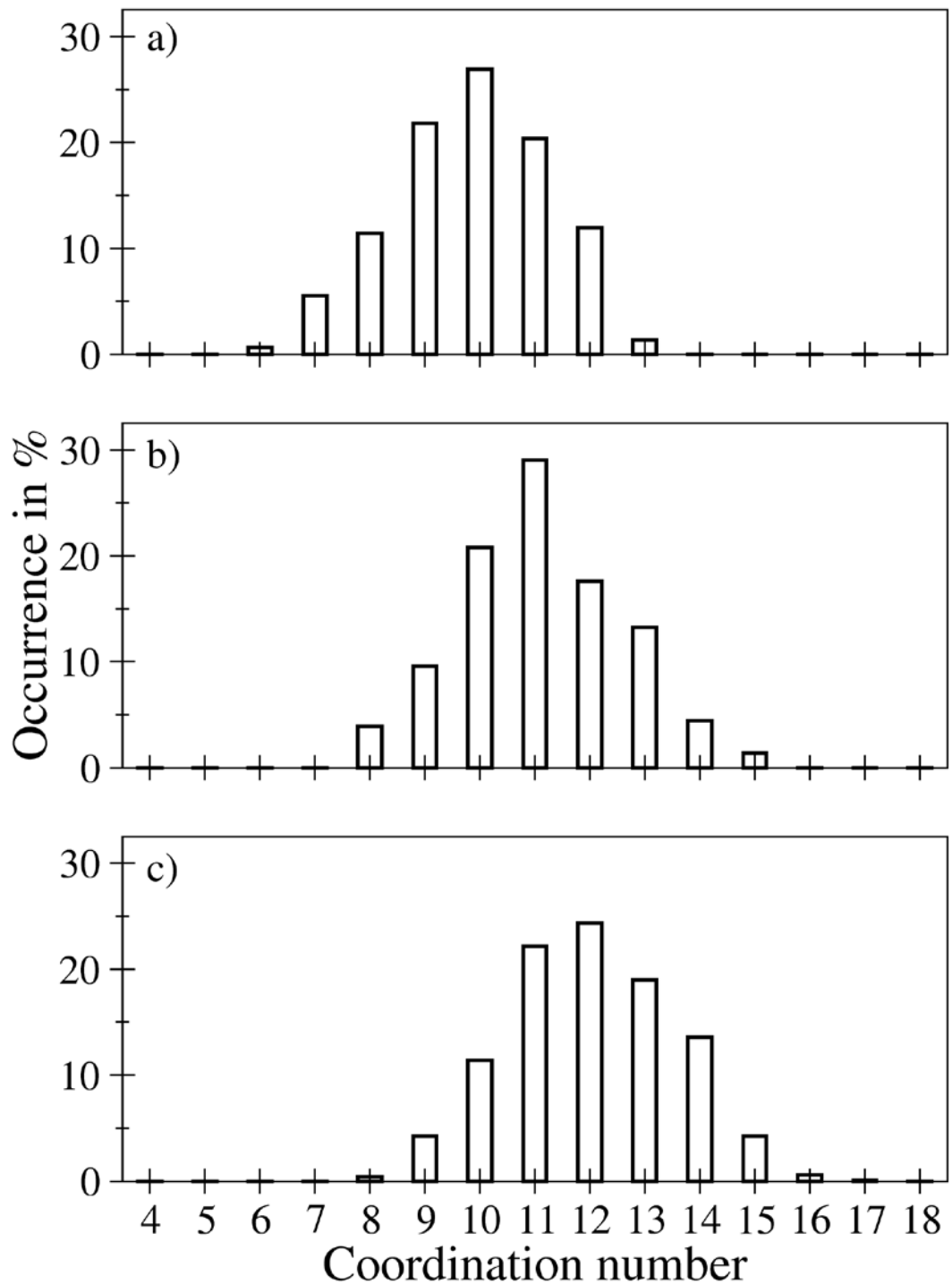


Figure 6

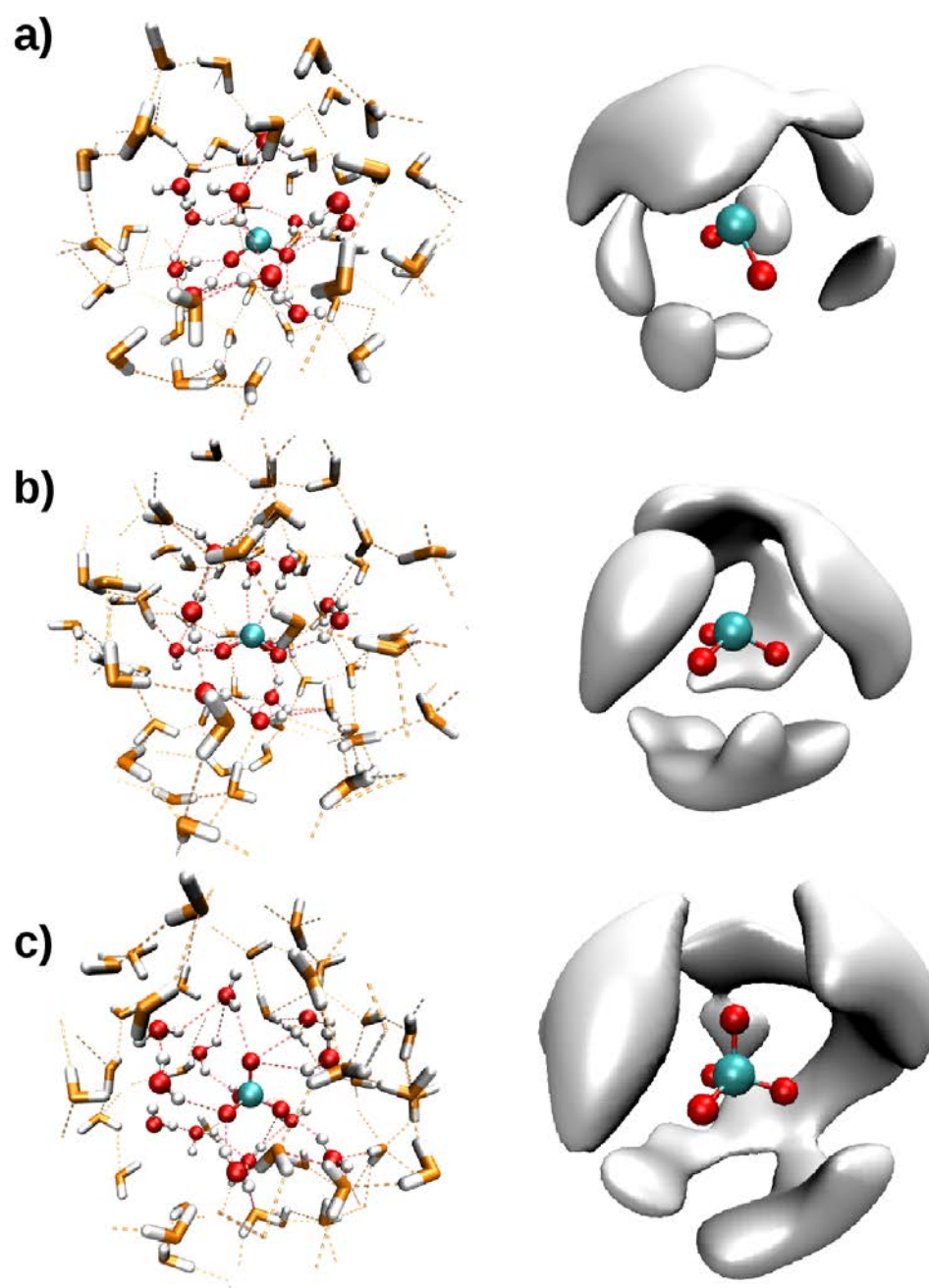


Figure 7

